

# Effect of polyimides with different ratios of *para*- to *meta*- analogous fluorinated diamines on relaxation process

Wenli Qu<sup>a</sup>, Tze-Man Ko<sup>a</sup>, Rohit H. Vora<sup>b,\*</sup>, Tai-Shung Chung<sup>a,b</sup>

<sup>a</sup>Department of Chemical and Environmental Engineering, National University of Singapore, 10 Kent Ridge Crescent, Singapore 119260

<sup>b</sup>Institute of Materials Research and Engineering, Polyimide Project Group: Advanced Polymers and Chemical Cluster, 3 Research Link, Singapore 117602

Received 29 September 2000; received in revised form 4 January 2001; accepted 1 February 2001

**Keywords:** Polyimide;  $\beta$ -relaxation; Dynamic mechanical analyzer and dielectric analyzer

## 1. Introduction

In recent years, as the electronic devices have become smaller with higher signal propagation, the requirements for the dielectric materials are much more stringent. Some aromatic polyimides possessing high glass transition temperatures, low coefficients of thermal expansion and low dielectric constants have been synthesized to satisfy the demands. In particular, fluorinated polyimides have received extensive attention due to their lower dielectric constants suitable for the microelectronic applications. Unfortunately, the use of most polyimides has been limited by their poor solubility. This means that the polyimides could not be directly processed in their imidized forms [1]. As a result, some polyimides with ‘hinges’ structure in the backbone were designed to improve the solubility at the expense of decreasing thermal stability and mechanical property. Therefore, it is important to investigate their relaxation properties while we consider the structure–property relationships of polyimides for specific application.

As is well known, most of aromatic polyimide and copolyimide films exhibit relaxation processes ( $\alpha$ ,  $\beta$ , and  $\gamma$  processes) in their dynamic mechanical and dielectric behaviors. At very low temperatures (around  $-80^{\circ}\text{C}$ ), a  $\gamma$  relaxation process normally called sub-ambient secondary relaxation can be observed in rigid aromatic polymers. It is associated with phenyl ring motions [2] and is influenced by moisture absorption content, aging history and morphology [3]. With temperature increasing, a subglass  $\beta$  relaxation process is observed in the range of  $50$ – $250^{\circ}\text{C}$  during the thermal treatment of polyimides. A  $\alpha$  relaxation process attributed to glass transition can be normally observed at high temperatures ( $>300^{\circ}\text{C}$ ). Its temperature and magnitude

are dependent upon the chain rigidity, ordered structure, and cooperativity of the segmental motion [4].

About the  $\beta$  relaxation, there are many proposed explanations, for example, Ikeda [5] suggested that the  $\beta$  relaxation be connected to the crystalline interplane slippage, which was observed in oriented films and not in unoriented molded samples. This explanation was in conflict with the crystallinity dependence of the magnitude of the  $\beta$  relaxation. There is another proposed explanation called ‘rotational vibrations’ in which Butta proposed that the main type of motion was rotational vibration of small segments of a chain around quasi-equilibrium positions. The motion of phenylene and imides rings contributed to this vibration [6]. Furthermore, Perena suggested that the mobility of phenylene groups in the diamines be involved in the  $\beta$  relaxation and subsegmental motion was responsible for the non-cooperative motion of  $\beta$  relaxation [7]. Sun [8] also reported that  $\beta$  relaxation related with rotation of rigid segments of *p*-phenylene and imide groups around hinges such as  $-\text{O}-$ ,  $-\text{CH}_2-$  and so on in diamines. On the other hand, dianhydrides can also affect the  $\beta$  relaxation process. The transition temperature of the  $\beta$  relaxation decreased with the incorporation of flexible linkages in the dianhydrides [9]. Hougham has studied the fluorination effect of the polyimide on the  $\beta$  relaxation. It is shown that  $\beta$  relaxation temperature shifted to higher temperatures with increasing fluorine weight percent in the diamine unit, with decreased glass transition temperatures [10]. Structure anisotropy such as chain orientation (both in-plane and deformation orientation) may serve as another factor that influences the  $\beta$  relaxation process. Arnold studied the crystallinity and orientation effects of the film on the  $\beta$  relaxation process in a series of segmented rigid-rod polyimide and copolyimide films through dynamic and mechanical behavior and computer modeling [4]. Li [9] also found that with the increase of the sizes and shape

\* Corresponding author. Tel.: +65-874-3326; fax: +65-872-0875.

E-mail address: rh-vora@imre.org.sg (R.H. Vora).

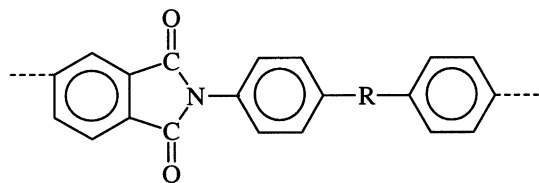


Fig. 1. Chemical structure presenting  $\beta$  relaxation schematization. R represents a flexible hinge such as O;  $\text{CH}_2$ ; S etc.

anisotropy of the disubstituted pendant groups at the 2- and 2'-position, the nature of the motion regarding to the  $\beta$  relaxation evolved from a non-cooperative process to a cooperative one. Fukami [11] have reported that compounds including *para*-phenylene or benzophenone groups in their chemical structure clearly showed the existence of a  $\beta$  relaxation. Habas [12] testified that there was a necessary condition for the existence of the relaxation  $\beta$ : the motions of *para*-phenylene and benzimide groups must be correlated. The chemical structure of showing a  $\beta$  relaxation is schematized in Fig. 1.

Although these explanations based on the experimental phenomenon can be used to illustrate some polymer relaxation process, sometimes they are not consistent with each other. Hence, much work need to be conducted to involve the effects of chemical structure and anisotropy by chain orientation induced during thermal imidization at the same time. In particular, the roles of chain rigidity and order to chain orientation are interesting subject in order to well understand relationships of structure and properties. Dynamic mechanical analyzer (DMA) and dielectric analyzer (DEA) can detect the change of chemical structure and anisotropy in polyimides. However, up to now it seems that no study has been reported about the effect of diamine analogous containing trifluorimethyl groups in fluorine copolyimide system. Therefore, the purpose of this study was to investigate the effects of different ratios of analogous diamines and anisotropy on the relaxation processes of copolyimide films. We expect that we could get some information of relaxation processes in diamine analogous copolyimides.

## 2. Experimental

### 2.1. Polymer synthesis

The copolyimides were synthesized from pyromellitic dianhydride (PMDA) dianhydride, 4,4'-(Hexafluoro-isopropylidene)dianiline (4,4'-6F) and 3,3'-(Hexafluoro-isopro-

pylidene)dianiline (3,3'-6F) diamine by two-step method. First, equivalent molar dianhydride was slowly added into the solution of mixed diamines in *N*-methyl-2-pyrrolidone (NMP) containing a certain molar percentage of analogous diamines, and was stirred for 24 h in nitrogen environment to get poly(amic acid) (PAA) solution [13]. Then, the PAA solution was spin coated onto the glass slides and thermally converted to copolyimide films using classical curing method. The acronym and structure of dianhydride and diamine are expressed in Scheme 1.

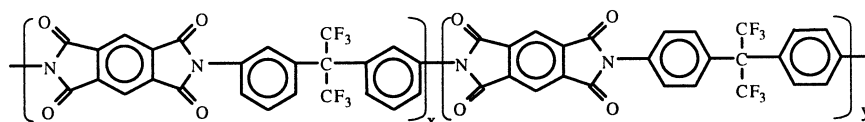
In this experiment, five different copolyimide compositions in the form of  $[(\text{PMDA} + 3,3'\text{-6F})_x + (\text{PMDA} + 4,4'\text{-6F})_y]$  were studied and simplified to CPI(0/100), CPI(85/15), CPI(75/25), CPI(65/35), and CPI(100/0). The film thickness was controlled between 40 and 50  $\mu\text{m}$  by spinning speed at 500 rpm for 30 s. Before the characterizations were performed, the films were dried in the oven overnight at 80°C and then put into the dessicator waiting for analysis.

### 2.2. Characterizations

Five kinds of PAA solutions inherent viscosities measured by Ubbelohde viscometer in 0.5 dl/g NMP at 20°C were 1.2947, 0.7196, 0.6845, 0.6022 and 0.7964, respectively. All of the polyimide film samples used for glass transition temperature ( $T_g$ ) measurements were heated at a rate of 10°C/min over the range of 30–400°C Netzsch Thermische Analyse DSC 200.

Dynamic mechanical properties were investigated at frequencies of 0.01, 0.1, 1, and 10 Hz, and at a ramping rate of 3°C/min over the range of 30–350°C in air by TA 2980 DMA. The films were cut into rectangular shape with 20 mm long and 4 mm wide, and then were mounted between two vertical clamps and a strain of 1% was applied in the dynamic measurements. Relaxation temperatures were obtained through the corresponding peak temperatures on the loss modulus ( $E''$ ) curves. And the  $\beta$  relaxation activation energy was calculated by using the Arrhenius equation, which is generally applied in the relaxation process related with the non-cooperative motions of small groups and fragments of the repeating unit. If the molecular motion becomes cooperative, the Arrhenius equation could not precisely describe the activation energy associated with the  $\alpha$  relaxation process. The activation energy of a single relaxation can be calculated by the slope of Arrhenius curve plotted by the logarithmic frequency,  $\ln(f)$ , versus the reciprocals of the relaxation peak temperatures determined from the loss modulus  $E''$  curve.

DEA 2970 Dielectric Analyzer (DEA) was used to investigate the dielectric properties and anisotropy of the



Scheme 1.  $[(\text{PMDA} + 3,3'\text{-6F})_x + (\text{PMDA} + 4,4'\text{-6F})_y]$ .

copolyimide films using single surface (in-plane) and two parallel sensors (out-of-plane) methods in nitrogen atmosphere at a frequency range of 1–100 kHz. For the in-plane dielectric property study, the film on the sensor was obtained by casting the PAA solution and then using classical curing method in an oven. After that, the sensor with a film on it was heated at a rate of 3°C/min in nitrogen from the room temperature to 350°C. For the out-of-plane dielectric study, the film was obtained from the conventional curing method. Then it was cut into 20 × 20 mm<sup>2</sup> piece and was sputter coated with a thin layer of gold on both sides for 40 s each in a chamber, which was evacuated to almost zero pressure and was backfilled with argon. The film was heated at a heating rate of 3°C/min in nitrogen between 30–350°C to detect the relaxation process by DEA. In this study, in order to illustrate the relaxation process, the plot of electric loss modulus  $M''$  against the temperature ( $T$ ) was used to describe the relaxation process. The same principle should be noted to the involved molecular cooperative motion.

X-ray diffraction (XRD) measurements were conducted at room temperature in reflection mode using a Shimadzu XRD-600 X-ray diffractometer. The Cu-K $\alpha$  radiation source ( $\lambda = 1.5418 \text{ \AA}$ ) was operated at 40 kV and 30 mA. The  $2\theta$  scan data were collected at 0.02° intervals over the range of 10–50° and the scan speed was 2 deg/min. The  $d$ -spacings corresponding to the large peak in the profile were calculated from Bragg's equation

$$\lambda = 2d \sin \theta,$$

where  $2\theta$  is the X-ray scattering angle,  $\lambda$ , the X-ray wavelength and  $d$  is the spacing.

Density of dry film was measured by AG204 Delta-Range Mettler Toledo with density determination kit. The film was cut into 30 × 20 mm. Before the measurement, the film was dried in vacuum oven overnight at 120°C to remove water absorbed. At the room temperature of 20°C, the weight of dry film was  $W_1$ , the weight of the dry film immersed in ethanol solvent was  $W_2$ , and ethanol solvent density at 20°C was 0.78934, the polyimide film density was obtained:  $\rho = W_1 / ((W_1 - W_2) / 0.78934)$ .

### 3. Results

#### 3.1. General properties of polyimide films

The solubility of PMDA-based polyimides was examined in tetrahydrofuran (THF), dimethylformamide (DMF), *N*-methyl-2-pyrrolidinone (NMP), and dimethylacetamide (DMAc). If 5 wt% concentration polyimide solution could be obtained, then it was considered that this kind of polymer is soluble in the solvent. It was observed that PMDA/3,3'-6F was not soluble in any solvent. With the introduction of 4,4'-diamine, the copolyimide CPI (85/15), CPI (75/25), and CPI (65/35) were

partly soluble in above organic solvents, while the molar ratio of 4,4'-6F increased to 100%, the polymer again did not fully dissolve in the solvent. The lower solubility of two homopolymers could be partially attributed to the rigid dianhydride structure in the backbone, which limited the chain packing. So these two polyimides show poor solubility. For the other three composition copolyimides, with *para* and *meta* catenation of two kinds of diamines along the polymer chains, the non-coplanar diamines disrupted the chain packing, eliminated crystallinity and interrupted conjugations along the chain backbones, the loose packing permitted the solvent molecules to penetrate through the polymeric chains, and finally resulted in better solubility than the homogeneous two polymers. These observed results about the two homogeneous polymer solubilities were consistent with the previous work done by many researchers [10]. It was observed that some polyimides showed lower solubility in common organic solvents because of rigid chains, such as Kapton (PMDA/ODA), Upilex (BPDA/PDA). This is also the reason that they are synthesized through two-step method and normally exist in PAA solution form, which is beneficial for further processing for specific application; while some polyimides show surprising solubility because of the incorporation of twisted-biphenyl diamines, such as PFMB, 2,2'-disubstituted groups in diamines [9]. And another factor towards increasing solubility was studied by Li F. et al. [15]. The solubility of 6FDA/PFMB was due to the asymmetric linkage and fluorinated isopropylidene group in 6FDA dianhydrides.

However, for our study, it is difficult to say how many of the diamine moieties improve the solubility because the copolymers exhibited the same solubility in the range of 35–65% molar ratio of 4,4'-6F diamine.

#### 3.2. Glass transition temperatures

DSC measurements were used to determine the  $T_g$ s of the polyimide films at a second heating (Fig. 2). From which a  $T_g$  of CPI(65/35) copolymer was obtained.  $T_g$ s of other

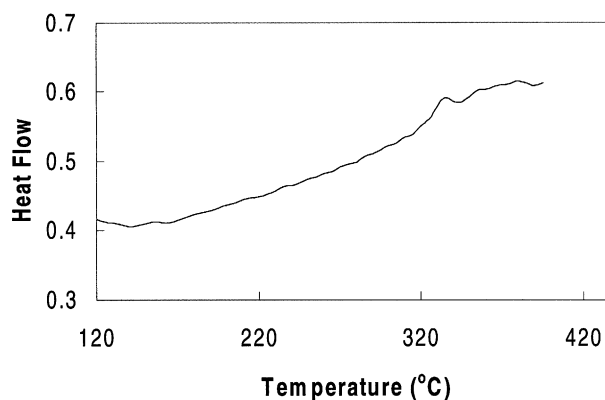


Fig. 2. DSC spectrum of CPI(35/65) film.

Table 1

Properties of various compositions of copolyimides [(PMDA + 3,3'-6F)<sub>x</sub> + (PMDA + 4,4'-6F)<sub>y</sub>]

PI film	$T_g$ (°C)	$d$ -spacing (Å)	Density (g/cm <sup>3</sup> )
CPI(100/0)	296	4.0	1.462
CPI(85/15)	311	3.9	1.454
CPI(75/25)	316	3.8	1.450
CPI(65/35)	329	3.7	1.454
CPI(0/100)	345	No	No

polyimides are listed in Table 1. It was observed that the glass transition temperature increased with increasing 4,4'-6F content in the copolymer system.

In order to testify the random copolymer system glass transition temperature validity, two equations are utilized: Fox's and DiMarzio–Gibbs's equations. These two equations are based on additivity rules, although with different theoretical backgrounds, namely free volume and conformational entropy.

The relationship between  $T_g$  and the weight ratio of the homo and copolyimide system is shown in fig. 3. The relationship was in agreement with Fox's equation [16] using weight fractions to predict the glass transition temperature

$$\frac{1}{T_g} = \frac{W_1}{T_{g1}} + \frac{W_2}{T_{g2}},$$

where  $T_{g1}$  and  $T_{g2}$  are the glass transition temperatures of the two homopolyimides, respectively;  $W_1$  and  $W_2$  are the weight ratios of homopolyimides, respectively;  $T_g$  is the glass transition temperature of a copolymer. This result suggests that copolyimides studied here were basically random copolymers.

Then DiMarzio–Gibbs's semi-empirical equation [17] was used to predict the change of  $T_g$  with composition in random copolymers.

$$T_g = m_1 T_{g1} + m_2 T_{g2},$$

where  $T_{g1}$  and  $T_{g2}$  are the glass transition temperatures of

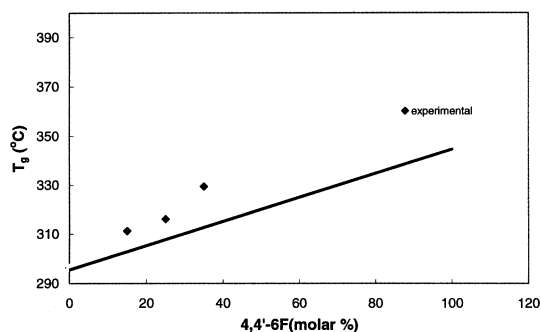


Fig. 3. Comparison of glass transition temperature of experimental data with calculated ones from DiMarzio–Gibbs's equation for polyimides with different 4,4'-6F diamine molar contents.

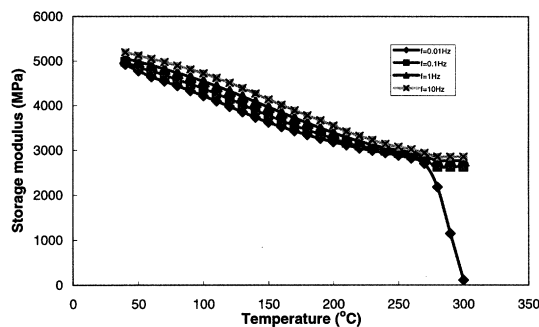


Fig. 4. Dynamic mechanical curves: storage modulus of PMDA/3,3'-6F at different frequencies.

homopolymers 1 and 2, respectively.  $T_g$  is the glass-transition temperature of a copolymer composed of two monomer units 1 and 2 with mole fractions  $m_1$  and  $m_2$ .

From the fitting curve, we obtained the same fitting using molar fractions and weight fractions due to the same molecular weight of 3,3'-6F and 4,4'-6F.

### 3.3. $\beta$ relaxation of polyimides measured by DMA

#### 3.3.1. $\beta$ relaxation

Work on  $\beta$  relaxation of polyimides has been studied widely. Fred E. Arnold et al. [4,18] systematically studied the origin of  $\beta$  relaxations in a series of segmented rigid-rod polyimide and copolyimide [(BPDA–PFMB)<sub>x</sub>–(PMDA–PFMB)<sub>y</sub>] films with different dianhydrides and diamines through DMA. For some of the polymers, crystallinity and orientation effects on the  $\beta$  relaxation process in the unoriented films can mainly be attributed to a relatively non-cooperative motion in uncrystallized diamines.

In our experiments, due to rigidity of CPI(0/100), it could not obtain uniform film for later relaxation analysis. So the final characterization is mainly on four kinds of polyimides. Our results on DMA also showed that  $\beta$  relaxation existed at different frequencies from both storage modulus and loss modulus ( $E''$ ). Figs. 4 and 5 displays the storage modulus and loss modulus change of CPI(100/0) as a function of temperature at frequency range of 0.01, 0.1, 1, and 10 Hz. A gradual decrease of the storage modulus was found when the temperature increased. From the loss modulus curve, relaxation process was clearly observed. It was also observed that at the relatively low frequency of 0.01, 0.1 and 1 Hz, a shoulder near the  $\beta$  relaxation existed. This might be associated with a separation of the molecular motion in the  $\beta$  relaxation in the low frequency region, and assigned as a  $\beta'$  relaxation. This might be the reason of a broader  $\beta$  relaxation peak temperature occurred. Recently, Li [9] assigned the relaxation as  $\beta_1$  relaxation and  $\beta_2$  relaxation processes.  $\beta_1$  relaxation was associated with a local motion related to the diamine constituent. While  $\beta_2$  relaxation was speculated to relate with the local motion of the dianhydrides. Therefore, polyimide films with fixed diamine should exhibit the same  $\beta_1$  relaxation

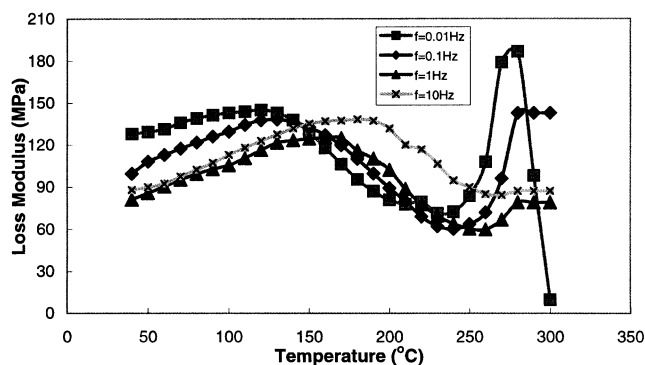


Fig. 5. Dynamic mechanical curves: loss modulus of PMDA/3,3'-6F at different frequencies.

behavior; when the dianhydride structure was the same in polyimide films, the  $\beta_2$  relaxation temperature should be constant. According to Li's report, here we also assigned the  $\beta$  relaxation as  $\beta_1$  relaxation and  $\beta_2$  relaxation processes in order to study the origin motion of polymers at low frequency. The  $\beta_1$  relaxation of CPI(100/0) at a frequency of 0.01 Hz occurred at around 105°C and at around 169°C at a frequency of 10 Hz. While the  $\beta_2$  relaxation of CPI(100/0) at a frequency of 0.01 Hz occurred at around 140°C and at around 191°C at a frequency of 10 Hz. It suggests the peak temperature of the  $\beta_1$ ,  $\beta_2$  relaxation was more sensitive to frequency. Fig. 6 shows the  $\tan \delta$  data of CPI(100/0) at four frequencies. The observed magnitude of  $\tan \delta$  for the  $\beta_2$  relaxations was about 0.03 in the frequency range from 0.01 to 10 Hz, not like  $\alpha$  relaxation, which had a broader range of magnitude.

Fig. 7 displays dynamic results measured at 1.0 Hz for a series of  $[(\text{PMDA} + 3,3'\text{-6F})_x + (\text{PMDA} + 4,4'\text{-6F})_y]$  films. It is clear that storage modulus ( $E'$ ) started decreasing in all kinds of polymer films during  $\beta$  relaxation process because of the temperature effect on the mobility of polymer chains. With temperature increasing, the mobility of chains increased and resulted in the storage modulus decreased.

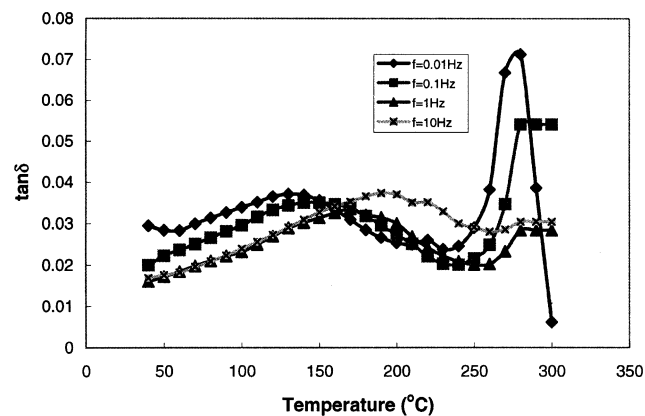


Fig. 6. Dynamic mechanical curves:  $\tan \delta$  of PMDA/3,3'-6F at different frequencies.

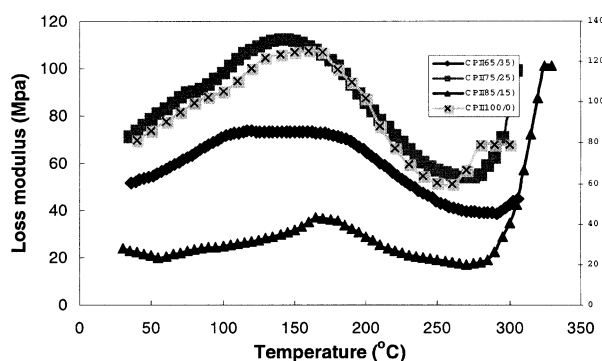


Fig. 7.  $\beta$  relaxation of four copolyimide films at a frequency of 1 Hz.

This is consistent with the findings of Butta [6] that the motion of phenylene and imides rings contributed to this vibration. From the loss modulus curve, which contained more broad  $\beta$  relaxation peak, a different  $\beta_1$  relaxation temperature and constant  $\beta_2$  relaxation temperature could be observed for four polyimide films at frequency of 1 Hz (Fig. 8(a)). This series of polyimide contained the same dianhydride PMDA with different ratios of *meta*- and *para*-diamines. The homopolymer CPI(100/0) film had higher peak temperature than that of two copolyimide films with the 4,4'-6F content less than 25% at frequency range of 0.01–10 Hz. This might be due to the decrease in the regularity leading to the decrease of intermolecular interaction, which in turn decreased the activation energy. In particular, with introduction of 4,4'-6F diamine to 35%,

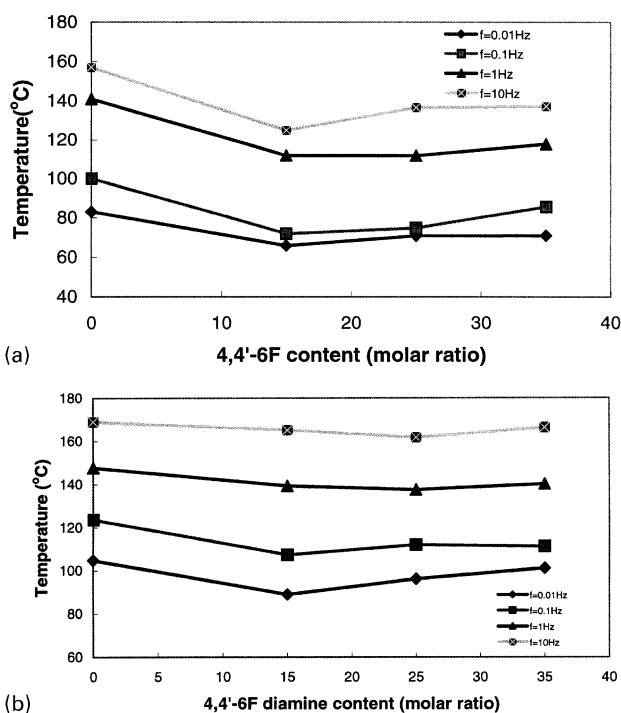


Fig. 8. (a)  $\beta_1$  relaxation temperatures of copolyimides versus 4,4'-6F molar content. (b)  $\beta_2$  relaxation temperatures of copolyimides versus 4,4'-6F molar content.

the rigid linkage in the main chain increased the packing force, which might predominate the disorder of the chain, so the  $\beta_1$  relaxation temperature shifted to higher temperatures. This conclusion was consistent with Li's experimental results of the DMB-based polyimide films and Arnold's report on [(BPDA-PFMB)<sub>x</sub>-(PMDA-PFMB)<sub>y</sub>] films, the  $\beta$  relaxation was independent of the copolymer composition in which diamine was fixed [4,15]. And it also exhibited that the existence of  $\beta$  relaxation had relation with *meta*-phenylene and benzimide groups.

It is evident from Fig. 8(b) that the  $\beta_2$  relaxation of homopolymer CPI(100/0) film had almost the same peak temperature as that of three copolyimide [(PMDA + 3,3'-6F)<sub>x</sub> + (PMDA + 4,4'-6F)<sub>y</sub>] films with the 4,4'-6F diamine content 0–35% at all frequencies in the range from 0.01 to 10 Hz. Based on these experimental results, we may conclude that the  $\beta_2$  relaxation was dependent on dianhydride and supported by the Li's and Coburn's reports [9,19].

### 3.3.2. Activation energy

As shown in Fig. 6, the  $\beta_1$ ,  $\beta_2$  relaxations of CPI(100/0) were sensitive to the frequency change. It demonstrated that the frequency-dependent  $\tan \delta$  changed with temperature at four frequencies. With the frequency increasing, the  $\beta_1$ ,  $\beta_2$  relaxation temperature would move toward higher temperature in accordance with Arrhenius' law. As the frequency increased, the lower temperature  $\beta_2$  relaxation began to merge with the  $\alpha$  relaxation. The  $\beta_1$ ,  $\beta_2$  relaxations were sensitive to frequency change due to its lower activation energy. The frequency dependence of the  $\beta_1$ ,  $\beta_2$  relaxation could be investigated using the Arrhenius equation, which can be successful in describing the temperature dependence for many thermal analysis systems. The Arrhenius equation (Eq. (1)) can be used to calculate the activation energy  $E_a$  of this relaxation, from peak temperatures at differing frequencies  $f$ .

$$f = A \exp(-E_a/RT), \quad (1)$$

here,  $A$  is the preexponential factor;  $R$  is gas constant.  $T$  is relaxation peak temperature;  $E_a$  is the activation energy.

The values of the activation energies of  $\beta_1$  and  $\beta_2$  relaxation had been determined by a curve fitting method [12]. The relationship of logarithmic frequency ( $\log f$ ) versus reciprocal transition temperature ( $1/T$ ) in  $\beta_1$ ,  $\beta_2$  relaxation process exhibited activation energies for homopolyimide  $142 \pm 5$ ,  $200 \pm 5$  kJ/mol and two copolyimides (with diamine content less than 25% molar in constituents)  $120 \pm 5$ ,  $200$  kJ/mol as shown in Fig. 9. The  $\beta_1$  relaxation processes for the homo or copolymers studied exhibited different  $\beta_1$  relaxation temperature and activation energies due to the PMDA/4,4'-6F introduction corresponding with frequencies. It indicated that diamine was contributed to the local motion of side groups in the system, even in the case of the same composition with different function group catenation- *para* or *meta*. It further induced that the  $\beta_1$  relaxation process was noncooperative, which implied that at low

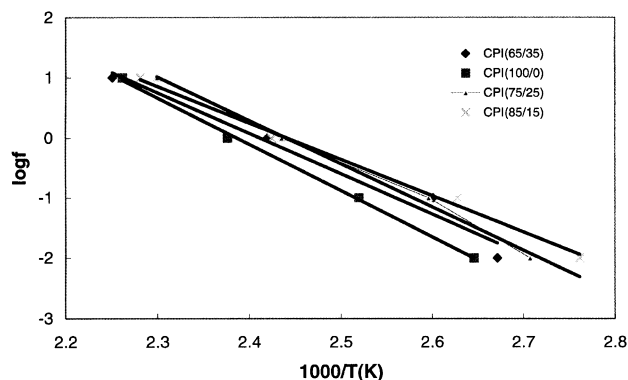


Fig. 9.  $\beta_1$  relaxation activation energies of [(PMDA + 3,3'-6F)<sub>x</sub> + (PMDA + 4,4'-6F)<sub>y</sub>] films.

temperature the activation entropies close to zero and the relaxation reflected motions of a distribution of segment lengths. Based on molecular modeling, the chain length between  $-C(CF_3)_2-$  and a phenyl group in a diamine moiety for 4,4'-6F was  $1.5 \text{ \AA}$ , respectively, while, for 3,3'-6F is  $1.51 \text{ \AA}$ . The bond angles of  $-C(CF_3)_2-$  in 4,4'-6F and 3,3'-6F were  $111.38^\circ$  and  $106.74^\circ$ , respectively [20].  $\beta_2$  relaxation was associated with dianhydride in the copolymer system, here, the dianhydride was fixed with PMDA in the copolymer system, the  $\beta_2$  relaxation almost kept constant at 200 kJ/mol. This  $\beta_2$  relaxation process caused by local motion of the dianhydrides was cooperative in nature. It was similar with Li's experimental results of the PFMB-based polyimide films which had  $E_a = 189$  kJ/mol for  $\beta_2$  relaxation process [9]. However, the  $\beta_2$  relaxation activation energy was higher than normal  $\beta$  activation energy, cooperative motion may involve in the systems.

In order to examine the data validity, it is necessary to apply theory method suggested by Starkweather [21] to identify the type of molecular motions involved in this process.

Eyring theory of absolute reaction rates was used in this calculation if the frequency-temperature dependence is of an Arrhenius type

$$f = \frac{kT}{2\pi h} \exp\left(-\frac{\Delta H^+}{RT}\right) \exp\left(\frac{\Delta S^+}{R}\right), \quad (2)$$

where  $k$  and  $h$  are the Boltzmann and Planck constants, respectively.  $R$  is the gas constant, and  $f$  is the frequency.  $\Delta S^+$  is the activation entropy.

The relationship between  $E_a$  and  $\Delta H^+$  is thus

$$E_a = \Delta H^+ + RT. \quad (3)$$

In Eq. (3), the Arrhenius activation energy  $E_a$  is

$$E_a = -Rd \ln f/d(1/T) \quad (4)$$

and the Eyring activation enthalpy  $\Delta H^+$  is

$$\Delta H^+ = -Rd \ln(f/T)/d(1/T). \quad (5)$$

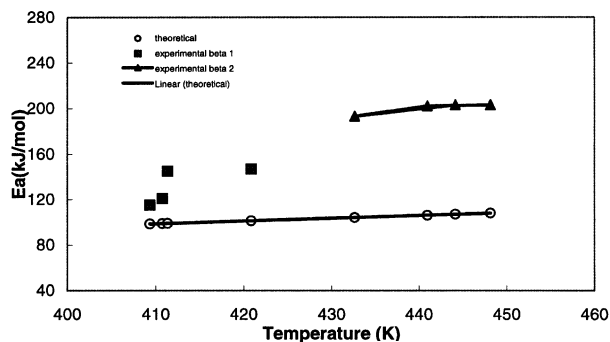


Fig. 10. Starkweather's plot of activation energies versus temperature.

Combining Eqs. (2) and (3), we obtain

$$E_a = RT[1 + \ln(k/2\pi h) + \ln(T/f) + T\Delta S^+]. \quad (6)$$

Starkweather reported that for many relaxation processes, particularly those involving small, submolecular fragments motions independent of one another, the activation entropy  $\Delta S^+$  is close to zero. Under this theory assumption, if the relaxation is at the frequency of 1 Hz at temperature  $T'$ , then  $E_a$  follows a simple, almost linear dependence on temperature

$$E_a = RT'[1 + \ln(k/2\pi h) + \ln T']. \quad (7)$$

The difference between the experimental  $E_a$  and this theory value is equal to  $T\Delta S^+$ . Eq. (7) defines an effective lower limit for the activation energies of viscoelastic relaxations [18].

From Eq. (7), we could calculate the activation energy,  $E_a$ . Fig. 10 shows the relationship between the activation energies of the  $\beta_1$  and  $\beta_2$  relaxation processes of this series polyimide films and temperature at 1 Hz. The solid line was the theoretical data based on Eq. (7). Under the assumption of  $\Delta S = 0$ , we obtained a value of 100 kJ/mol for  $\beta_1$  relaxation, which was attributed to the local motion of diamines. The data obtained from Arrhenius experimental equation fell right above the solid line, nearer to the line, not like the  $\beta_2$  relaxation far deviating from the non-cooperative motion. Hence, It suggests that for the  $\beta_2$  relaxation the

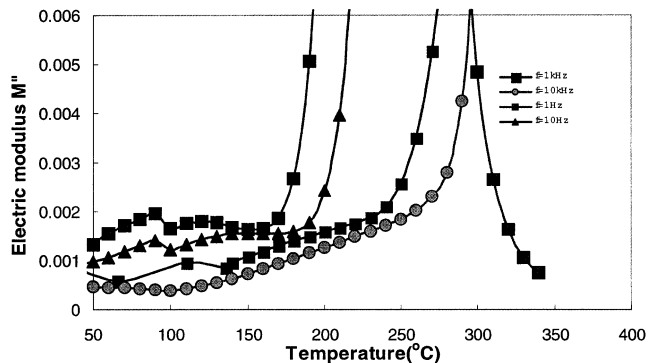


Fig. 12. Electric modulus of CPI(100/0) at four frequencies.

assumption of  $\Delta S = 0$  might not be very precise and the motion in this process must be lower non-cooperativity in nature, and no longer a single relaxation process.

This origin of  $\beta$  relaxation process of  $[(\text{PMDA} + 3,3'-6\text{F})_x + (\text{PMDA} + 4,4'-6\text{F})_y]$  was not like that of PMDA-ODA film. And the detailed nature of this motion in the  $\beta$  relaxation has not been well characterized. It needs to study more from experimental and theory point. Perhaps high-temperature  $^{13}\text{C}$  solid-state NMR measurements could help to identify this kind of motion.

### 3.4. $\beta$ relaxation of polyimide films by DEA

It is shown that the dynamic mechanical measurement only covered a relatively narrow frequency region. Hence, the dielectric experiment was also performed in order to study the relaxation behaviors of these polyimide films over a wider frequency region to 100 kHz.

As mentioned before, a similar observation can also be found in the DEA experiments from parallel thin film sensor (out of plane direction) as shown in Fig. 11 at two frequencies of 10 and 100 kHz. Both the permittivities and loss factors for the CPI(75/25) manifested the existence of  $\beta_1$  and  $\beta_2$  relaxation processes in the kHz-range. It is noted that this kHz-range measurements were representative of the rearrangement of dipoles of the polymer chain

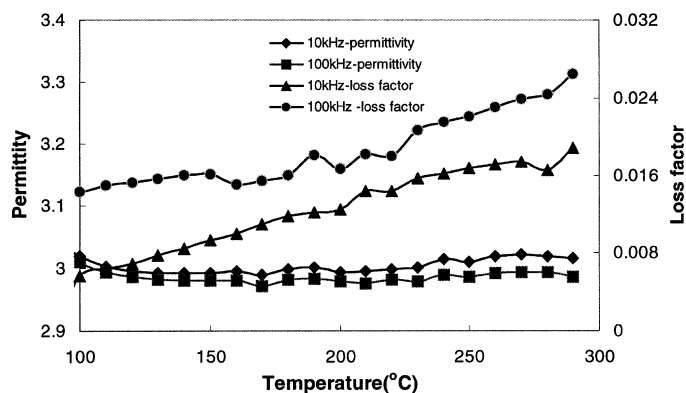


Fig. 11. DEA experimental results of CPI(75/25) at high frequencies.

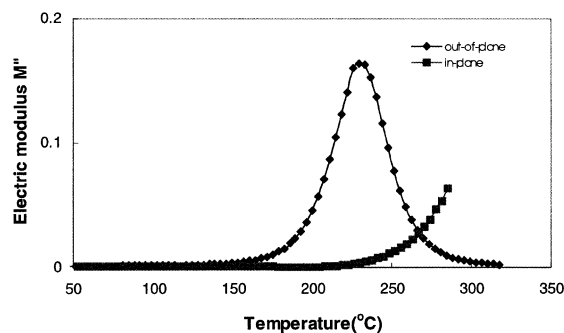


Fig. 13. Electric loss modulus  $M''$  of CPI(75/25) along the in-plane and out-of-plane directions at 1 Hz.

molecules under an electric field [22]. To better illustrate the relaxation process, the electric modulus was used, it is defined as the  $\epsilon''/(\epsilon'^2 + \epsilon''^2)$  [23]. Fig. 12 shows the electric loss modulus changed at different frequencies for PMDA/3,3'-6F. It is interesting to see that a  $\beta_1$  and  $\beta_2$  relaxation could be observed along the out-of-plane direction at lower frequencies. Since lower activation energy was needed for this relaxation process, it was sensitive to the frequency changes and at higher frequencies around 10 kHz, the  $\beta$  relaxation process became broader. Combining the DMA and DEA data, and plotting the Arrhenius relationship, their data were so close to each other and fitted well in one linear line about activation energies of  $\beta_1$  and  $\beta_2$  relaxations, (Figs. 8a, b). Hence, here it is not explained in detail.

It is clearly shown in Fig. 13 that there was a difference between the in-plane and out-of-plane  $\alpha$  relaxations. It reflected the glass transition process. Furthermore, the  $\beta_1$  and  $\beta_2$  relaxations could be observed from the curves, and the relaxation temperature of in-plane also was higher than that of out-of-plane direction. It suggests that there existed anisotropy in this polymer system.

### 3.5. Orientation effect on $\beta$ relaxation

To relate structure with relaxation behavior of  $[(\text{PMDA} + 3,3'\text{-6F})_x + (\text{PMDA} + 4,4'\text{-6F})_y]$  films, X-ray diffraction measurements were conducted at room temperature in reflection mode. As we know, the reflection mode runs in which the diffraction vector is in the direction normal to the film plane, providing structural information in the direction of film thickness. The reflection X-ray diffraction results of copolymer film CPI(65/35) are illustrated in Fig. 14. The reflection pattern revealed structureless X-ray diffraction patterns. It showed one broad amorphous halo at around  $23.8^\circ$ , corresponding to a  $d$ -spacing of  $3.7 \text{ \AA}$  calculated by Bragg's equation. The absence of the  $(00l)$  peaks indicated that the polymer chains were preferentially aligned in the film plane. Furthermore, no appearance of  $(hkl)$  peaks suggested that the polymer chains aligned in the film plane are packed without any regular ordering. It might result from poor chain ordering caused by the bulky di(trifluoromethyl) groups. Hence, this

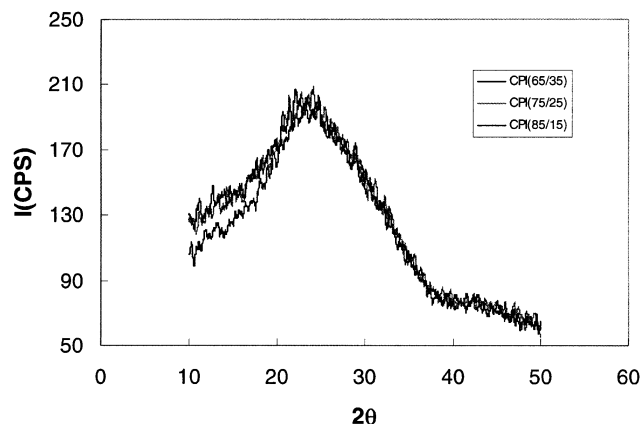


Fig. 14. XRD spectrum of three copolyimide films.

molecular in-plane orientation detected on the X-ray pattern was directly correlated to the dielectric anisotropy discussed in Section 3.4. This  $d$ -spacing was almost the same as that of the other two copolyimides CPI(75/25) and CPI(85/15) with  $d$ -spacing of  $3.8$  and  $3.9 \text{ \AA}$ , while smaller than that of homopolymer CPI(100/0) with  $4.0 \text{ \AA}$  distance. So the mean intermolecular distance, which is a parameter of molecular packing, is in the increasing order  $\text{CPI}(65/35) \leq \text{CPI}(75/25) \leq \text{CPI}(85/15) < \text{CPI}(100/0)$ . This result, in turn, could illustrate that *para*-diamine introduction reduced steric bulkiness, resulting in efficiency molecular packing. Turning to the orientation effect on this relaxation, it is evident that with increasing the 4,4'-6F content and with decreasing the  $d$ -spacing,  $\beta_1$  relaxation temperature of copolyimide films shifted toward higher temperatures for CPI(65/35) than the other two copolyimide films. It is to note that  $\beta_1$  relaxation temperature of CPI(100/0) was higher than the copolyimide films, it might be due to the in-plane ordering of polymer chains, it need to be further studied by transmission mode of WAXD measurement.

In order to test the result exactness about  $\beta_1$  relaxation process, density measurements were also conducted at temperature of  $20^\circ\text{C}$ . The data was shown in Table 1, it showed that density of CPI(100/0) was slightly higher than that of other three copolymer films. Moreover, it indicated that the  $\beta_1$  relaxation of homopolymer had higher relaxation temperature, and with introduction of *para*-diamine to 35 molar percent, the relaxation temperature are almost the same as the homopolymer.

## 4. Conclusion

In this experiment, the five different compositions of copolyimides in the form of  $[(\text{PMDA} + 3,3'\text{-6F})_x + (\text{PMDA} + 4,4'\text{-6F})_y]$  were mainly characterized by dynamic mechanical property at a heating rate of  $1^\circ\text{C}/\text{min}$  at four frequencies (0.01, 0.1, 1, and 10 Hz) and dielectric properties by single surface sensor (in-plane direction) and thin film parallel plate sensor (out-of-plane direction)



measurement. The solubility of copolyimides is better than the homo polymers. The  $\beta$  relaxations of four polyimides showed similar trends:  $\beta_1$  and  $\beta_2$  relaxations, which occurred around 105, 140°C at a lower frequency of 0.01 Hz and 169, 191°C at 10 Hz for PMDA/3,3'-6F, and had activation energies about  $140 \pm 5$ ,  $200 \pm 5$  kJ/mol, respectively. With the introduction of 4,4'-6F diamine, the  $\beta_1$  relaxation temperature slightly decreased until its molar content up to 35%, the rigidity and steric hindrance overcame the disorder caused by copolymerization and kept almost the same packing coefficient confirmed by X-ray diffraction and density measurement. However, for the  $\beta$  relaxation process, the motion showed there was a little difference from the previous study, in which there is only one  $\beta$  relaxation by small segment motion in polymer backbone. Our experiment results indicated that  $\beta_1$  relaxation was related with diamine in the polyimide system; while  $\beta_2$  relaxation was independent on diamine. And dianhydride contributed to the  $\beta_2$  relaxation process, which was slightly cooperative motion in the polymer system. At the same time, X-ray diffraction and density measurements were carried out on relate structure with relaxation behavior of these PI films. It further illustrated that the *para*-diamine introduction reduced steric bulkness caused by *meta*-diamine connection, resulting in efficient molecular packing with decreasing *d*-spacings and increasing density for  $[(\text{PMDA} + 3,3'\text{-6F})_x + (\text{PMDA} + 4,4'\text{-6F})_y]$ .

## References

- [1] Jeon JY, Tak TM. J Appl Polym Sci 1996;61:529.
- [2] Habas JP, Peyrelasse J, Grenier-Loustalot MF. High Perform Polym 1996;8:515.
- [3] Jonas A, Legras R. Macromolecules 1993;26:813.
- [4] Arnold Jr FE, Brono KR, Shen DX, Eashoo M, Lee CJ, Harris FW, Cheng SZD. Polym Engng Sci 1993;33:1373.
- [5] Ikeda RM. J Polym Sci, Polym Lett Ed 1966;4:353.
- [6] Butta S, Petris SD, Pasquoni M. J Appl Polym Sci 1969;13:1073.
- [7] Kim YH, Moon BS, Harris FW, Cheng SZD. J Therm Anal 1996;46:921.
- [8] Sun ZH, Dong LS, Zhuang YG, Cao LY, Ding MX, Feng ZL. Polymer 1992;33:4728.
- [9] Li FM, Fang S, Ge JJ, Honigfort PS, Chen JC, Harris FW, Cheng SZD. Polymer 1999;40:4987.
- [10] Hougham G, Tesoro G, Shaw J. Macromolecules 1994;27:3642.
- [11] Fukami A, Iisaka K, Kubota S, Etoh S. J Appl Polym Sci 1991;42:3065.
- [12] Habas JP, Peyrelasse J, Grenier-Loustalot MF. High Perform Polym 1996;8:515.
- [13] Vora RH, US Patent Y.933,132.
- [15] Li F, Fang S, Ge JJ, Honigfort PS, Chen JC, Harris FW, Cheng SZD. Polymer 1999;40:4571.
- [16] Yin J, Ye Y-F, Li L, Zhang Y-L, Huang Y, Wang Z-G. Eur Polym J 1999;35:1367.
- [17] DiMarzio EA, Gibbs JH. J Polym Sci 1959;40:121.
- [18] Arnold Jr FE, Shen DX, Lee CJ, Harris FW, Cheng SZD, Starkweather Jr HW. J Mater Chem 1993;3:183.
- [19] Coburn JC, Soper PD, Auman BC. Macromolecules 1995;28:3253.
- [20] Chung TS, Vora RH, Jaffe. J Polym Sci, Part A: Polym Chem 1991;29:1207.
- [21] Starkweather Jr HW. Polymer 1991;32:2443.
- [22] Cheng SZD, Chalmers TM, Gu Y, Yoon Y, Harris FW. Macromol Chem Phys 1995;196:1439.
- [23] Starkweather Jr HW, Avakian P. J Polym Sci B: Polym Phys 1992;30:637.